Evolution of the electronic properties of small Ni_n^- ($n=1-100$) clusters by photoelectron spectroscopy

Shu-Rong Liu, Hua-Jin Zhai, and Lai-Sheng Wang[a)]
Department of Physics, Washington State University, Richland, Washington 99352 and
W. R. Wiley Environmental Molecular Sciences Laboratory, Pacific Northwest National Laboratory, MS K8-88, Richland, Washington 99352

(Received 14 August 2002; accepted 13 September 2002)

Photoelectron spectra of size-selected and relatively cold Ni_n^- ($n=1-100$) clusters were obtained at three detachment photon energies; 355, 266, and 193 nm. The evolution of the electronic structure of Ni_n^- clusters from molecular to bulklike behavior was systematically investigated. Well-resolved threshold peaks were observed for small Ni_n^- clusters ($n\leqslant 9$), beyond which a single broadband was observed due to the high electronic density of states at large cluster sizes. This spectral change coincides with a dramatic decrease of the magnetic moment in this size range. In addition, narrow and well-resolved spectral features were observed around $n=13$ and 55, consistent with high symmetry icosahedral structures proposed for these clusters. A sharp threshold peak was observed in the spectra of Ni_{19}^- and Ni_{23}^-, also evident of more symmetric cluster structures. The spectra of Ni_3^- measured at various photon energies suggested the existence of two isomers. The electron affinities of the Ni_n clusters were observed to follow the prediction of a metallic droplet model at large cluster sizes above $n=10$ and extrapolate to the bulk work function of Ni at infinite size.
 [DOI: 10.1063/1.1519008]

I. INTRODUCTION

One of the most interesting issues in cluster science is how cluster properties change as a function of size. The physical and chemical properties of clusters, such as their magnetism and chemical reactivity, are determined by their underlying geometric and electronic structures. Therefore, studies on the geometric and electronic structures are essential to understand the various properties of clusters. However, the determination of the atomic arrangements in transition metal (TM) clusters still remains challenging. Among the $3d$ TM clusters, Ni systems have received the most attention both experimentally and theoretically.[1–49] Riley and co-workers,[1–10] using the chemisorption method, have extensively investigated the structural properties of Ni clusters and proposed icosahedral packings in certain size ranges. An icosahedral shell structure for large Ni clusters in the size range between 50–800 atoms was also suggested through a near-threshold photoionization experiment.[11] Furthermore, the magnetic properties of Ni clusters have been studied by the Stern–Gerlach technique.[12–15] Small Ni clusters containing a few to hundreds of atoms were shown to possess larger magnetic moments than bulk Ni. In general, the magnetic moment per Ni atom decreases with increasing cluster size and approaches the bulk value for clusters containing about 700 atoms. There have also been extensive theoretical works on the energetics, equilibrium geometries, electronic structures, and magnetic moments of Ni clusters.[23–44] Icosahedral structures have been obtained consistently for the so-called magic numbers Ni_{13} and Ni_{55}.

Photoelectron spectroscopy (PES) of size-selected anions is a valuable technique to obtain electronic structure information for TM clusters. It provides directly the valence electronic density of states of the neutral clusters. The electronic structure information available from PES data can also provide insight into the structural, magnetic, and chemical properties of clusters. Several PES studies have been reported previously on small Ni_n^- clusters.[45–48] On the basis of the similarity of the PES spectra between Cu_n^- and Ni_n^- ($n\leqslant 7$), it was suggested that the enhanced magnetic moments are due to the localization of the $3d$ electrons and the lack of $s-d$ hybridization in the small cluster size regime.[45] High-resolution PES spectra were reported for Ni_2^- and Ni_3^- at low photon energies.[47,48] We have previously studied Ni_n^- clusters and presented well-resolved PES spectra for $n=1-50$. In particular, spectroscopic evidence was provided for a high symmetry icosahedral structure for Ni_{13}^-.[46]

In the current paper, we report a more comprehensive PES study on the Ni clusters. We have obtained PES data for Ni_n^- for n up to 100 under well-controlled temperature conditions and three photon energies: 355 nm (3.496 eV), 266 nm (4.661 eV), and 193 nm (6.424 eV). The evolution of the electronic structure as a function of size is systematically probed. The more complete PES dataset also affords us the opportunity to compare with a number of other experimental studies. We observed PES spectral changes in size regimes where changes in chemical and magnetic properties were also previously observed. In particular, sharp spectral features were observed for clusters at $n=13$, 19, 23, and 55, consistent with the icosahedral or polyicosahedral structures proposed previously for these clusters.

a)Electronic mail: ls.wang@pnl.gov

II. EXPERIMENT

The experiment was performed using a magnetic-bottle time-of-flight photoelectron spectroscopy apparatus with a laser vaporization supersonic expansion cluster beam source. Details of the apparatus were reported elsewhere.[50,51] In the current study, a pure Ni disk target was vaporized by a pulsed laser beam from a Nd: YAG laser. The laser-generated plasma was mixed with a high-pressure helium carrier gas pulse. Clusters formed in the nozzle were entrained in the carrier gas and underwent a supersonic expansion. Negatively charged clusters in the beam were extracted perpendicularly into a time-of-flight mass spectrometer. A given cluster of interest was mass selected and decelerated before photodetachment using either a Nd:YAG laser (355 and 266 nm) or an ArF eximer laser (193 nm). In the current study, several improvements were made. First, the instrumental resolution was slightly improved to about 2.5% ($\Delta E_k/E_k$), i.e., about 25 meV for 1 eV electrons, as measured from the known spectra of Rh^-. Second, we obtained data at various photon energies, 355, 266, and 193 nm. Low photon energy spectra provided better-resolved data for low binding energy features, while the high photon energy data allowed us to probe more deeply into the valence band of the clusters. Third, we extended the cluster size up to $n=100$ by fully optimizing the source conditions and the mass spectrometer. Finally and most importantly, we obtained data under well-controlled temperature conditions.

Good instrumental resolution and cold anion clusters are both crucial to resolve the intrinsic electronic features of clusters in PES experiments. Hot clusters, in general, result in severe spectral broadening that smears out discrete electronic transitions even under a high instrumental resolution. As shown previously for an Al_n^- clusters,[52] cluster temperatures from our cluster source span a wide range from as low as 250 K to more than 1000 K, depending on the residence time of the clusters in the nozzle and the firing timing of the vaporization laser.[53] In general, colder clusters were produced for a longer residence time in our source. Figure 1 shows the 355 nm spectra of Ni_n^- ($n=7$, 8, 9, and 13) at two conditions. The ''hot'' spectra were measured for clusters with a shorter residence time in the nozzle, whereas the ''cold'' spectra were taken for clusters with a longer residence time. Clearly better resolved features were obtained for colder clusters, even though the instrumental resolution remained the same. Especially, for Ni_8^- and Ni_9^-, the sharp threshold peak was almost smeared out for hot clusters, but well resolved under cold conditions. It is also important to note that the low-energy tail due to hot band transitions was considerably reduced in the cold spectra, giving rise to well-defined detachment thresholds and more accurate values for the electron affinities (EAs).

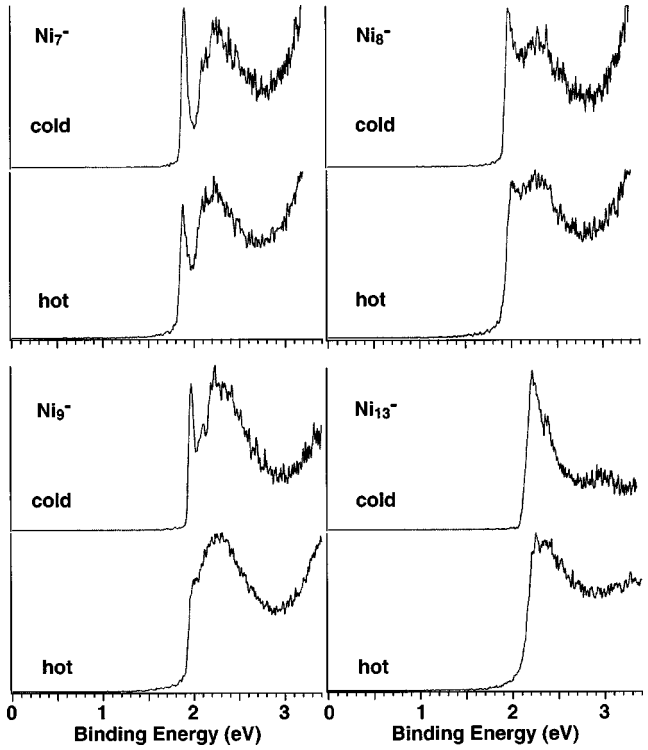

FIG. 1. Photoelectron spectra of Ni_n^- ($n=7-9$, 13) at 355 nm, measured at two temperature regimes (see the text).

III. RESULTS

A. 355 nm spectra: Ni_n^- ($n=1-32$)

The 355 nm spectra of Ni_n^- ($n=1-32$) are shown in Fig. 2. Note the different binding energy ranges plotted in each column. Compared to PES spectra reported previously,[45,46] the current data show much better resolved features and well-defined threshold with negligible hot band tails on the low binding energy side. For small clusters with $n=1-6$, the PES spectra exhibit strong size dependence with no resemblance to each other. These clusters are essentially molecular like. The spectrum of the atomic anion Ni^- shows a main peak at 1.11 eV, which is dominated by detachment transitions from the anionic ground state to the ^3D_j states of the Ni atom.[54] The spectrum of Ni_2^- shows a strong band located at 0.9 eV and a high density of states in the higher binding energy range. This spectrum is consistent with those previously reported.[45–47] The spectrum of Ni_3^- is unusual, showing features at around 1.5 eV with very low intensity and intense features between 2.2–3.5 eV. The spectra of Ni_6^- to Ni_9^- are similar; each possess a well-resolved sharp threshold peak and a broadband at higher binding energies. With the increase of cluster size, the energy separation between the sharp peak and the broadband decreases. Starting from Ni_{10}^-, the sharp peak merges with the broadband and could not be resolved.

The spectra of Ni_{11}^- and Ni_{12}^- are broad similar to that of Ni_{10}^-, except that the spectrum of Ni_{12}^- seems to show some noticeable fine features. From Ni_{12}^- to Ni_{13}^-, the spectrum undergoes a certain change to become much narrower. From Ni_{14}^- to Ni_{21}^-, the spectra remain similar to that of Ni_{13}^-, but gradually broaden, except that the spectrum of Ni_{19}^- seems to exhibit a unresolved threshold peak. The spectra of Ni_{22}^- to Ni_{26}^- each show a resolved peak at the threshold, which is particularly distinct in the spectrum of Ni_{23}^-. From Ni_{27}^- to Ni_{32}^-, a single PES band was observed at 355 nm with the exception of the spectrum of Ni_{28}^-, which displays a weak peak at its threshold.

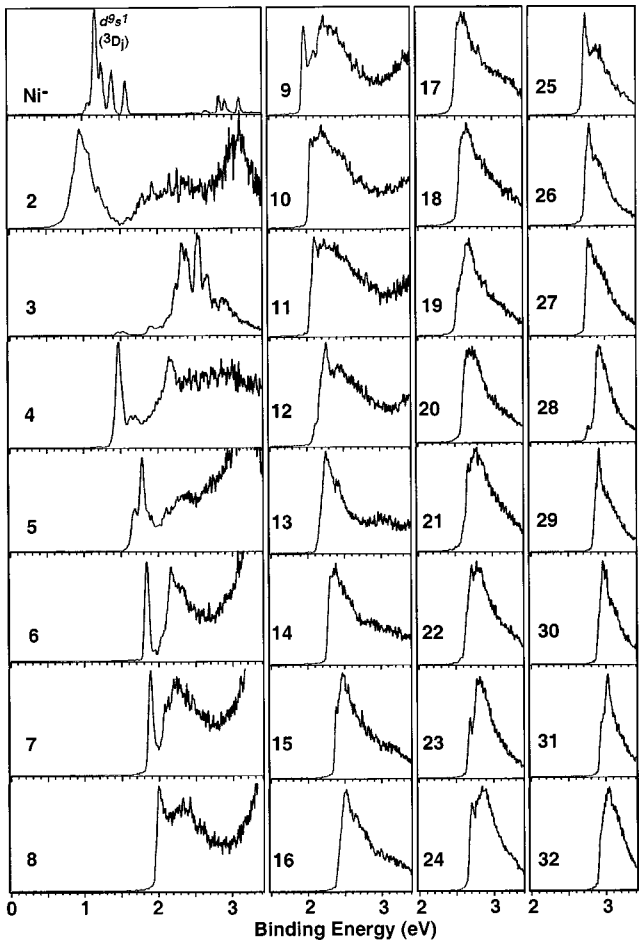

FIG. 2. Photoelectron spectra of Ni_n^- ($n=1-32$) at 355 nm (3.496 eV). Note the different ranges of binding energies plotted in each column.

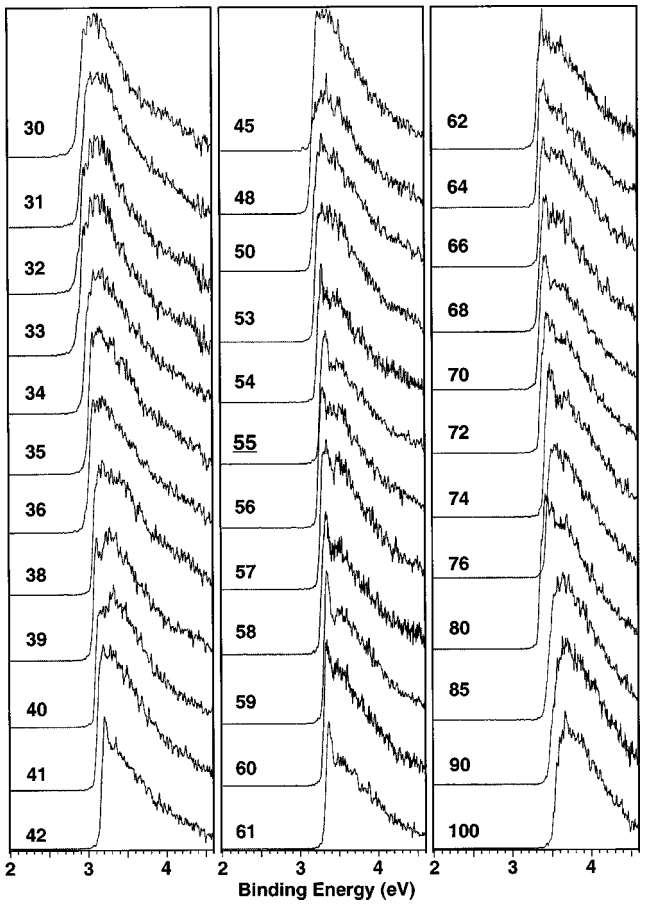

FIG. 3. Photoelectron spectra of Ni_n^- ($n=30-100$) at 266 nm (4.661 eV).

B. 266 nm spectra: Ni_n^- ($n=30-100$)

The 266 nm spectra of Ni_n^- ($n=30-100$) are shown in Fig. 3. Note that the binding energy range plotted is from 2.0 to 4.6 eV. We did not take the 266 nm spectra for small Ni_n^- clusters with $n<30$, because no new spectral information could be revealed due to the spectral congestion. Basically, a single broad and featureless band was observed for all clusters in this size range at this photon energy, except for Ni_{54}^- to Ni_{61}^-, for which a sharp peak was resolved surprisingly in the threshold regime. In particular, the spectra of Ni_{55}^-, Ni_{59}^-, and Ni_{61}^- each possess a well-resolved threshold peak. Comparing the spectra of Ni_{30}^- to Ni_{32}^- at 355 and 266 nm, we found that only the threshold region was observed in the lower photon energy spectra, which were much better resolved. A small shoulder was even observed in the 355 nm spectrum of Ni_{31}^-, which could not be resolved in the 266 nm data. Clearly, the broadband observed for the large clusters is a direct reflection of their high density of electronic states.

C. 193 nm spectra

Figure 4 shows the spectra of Ni_n^- ($n=3-60$) at 193 nm for a set of selected clusters. The spectral resolution deteriorated considerably at this high photon energy. The sharp threshold feature resolved in the 355 nm spectra for small clusters ($n=4-9$) became shoulders in the 193 nm spectra. Continuous signals were observed in the high binding energy side without any well-defined features for all the clusters, again indicating the high density of electronic states in these clusters. No additional spectral information was obtained in the 193 nm data; thus larger clusters were not investigated at this photon energy.

D. Photon energy-dependent PES spectra

The PES spectra of Ni_4^- to Ni_7^- at three photon energies are compared in Fig. 5. These spectra show more clearly the dependence of photodetachment transitions on photon energies. The PES peak intensity is directly related to the detachment cross section for a given detachment channel. Since photodetachment cross sections from different electrons (*s*, *p*, or *d*) show different photon energy dependence,[55] the peak intensity change can provide additional information about the nature of the PES features. For the spectra presented in Fig. 5, we see that the threshold sharp peaks all decrease in intensity as the photon energy increases, whereas the relative intensity of the broadband at higher binding energies all increases.

E. Adiabatic electron affinities

The adiabatic detachment energies or the electron affinities (EAs) for the neutral clusters were estimated from the 355 nm spectra for $n=3-32$ and the 266 nm spectra for *n*

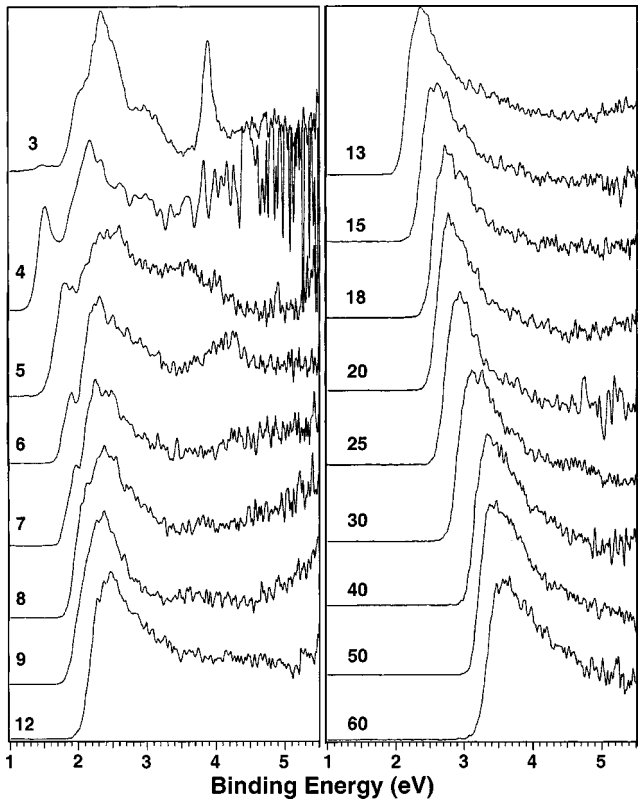

FIG. 4. Photoelectron spectra of Ni_n^- ($n=3-60$) at 193 nm (6.424 eV).

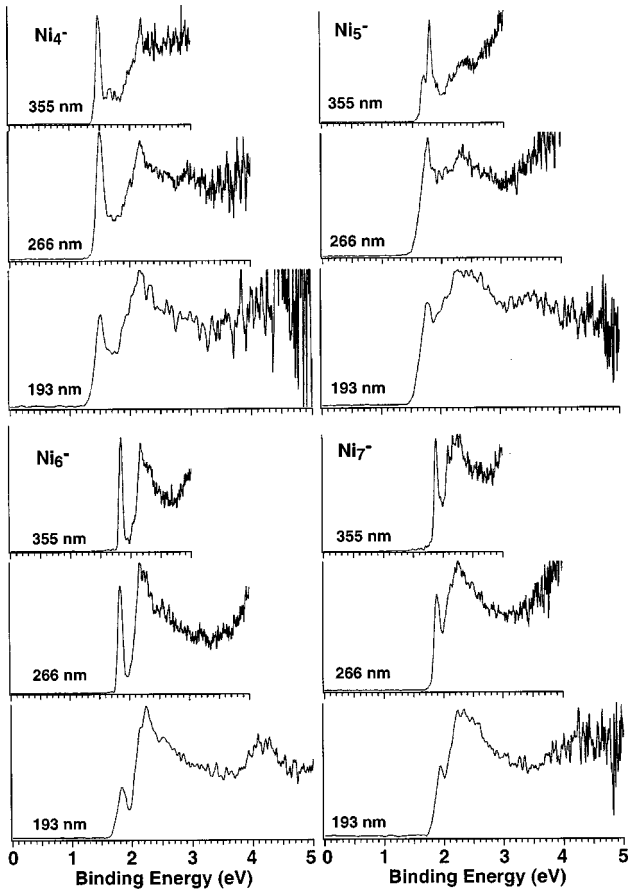

FIG. 5. Photon-energy-dependent spectra of Ni_n^- ($n=4-7$).

$=33-100$ and are presented in Table I. Because no vibrational structures were resolved, the EAs were evaluated by drawing a straight line at the leading edge of the PES spectra and then adding a constant of $\sim 0.02-0.04$ eV to the intersection with the binding energy axis to take into account the instrumental resolution. Although this is an empirical and approximate procedure, reasonably accurate and consistent EAs were obtained, particularly for PES spectra with sharp onsets. Within the experimental uncertainty, the currently obtained values are in agreement with our previous results in the size range of Ni_3 to Ni_{50}.[46]

The relatively cold cluster anions and the improved spectral resolution allowed sharp PES onset to be observed in all of the spectra for Ni_n^- (except for Ni_3^-; see below), largely due to the reduction of hot band transitions, which tend to result in low-energy tails, as illustrated in Fig. 1. In an extreme case, we have shown,[56,57] through temperature-dependent studies,[52,53] that the EA of Al_{13} is 3.57 ± 0.05 eV, a very high value reflecting the magic nature of Al_{13} as a 39-electron system, one short of the 40 electrons needed to form the closed shell Al_{13}^-. This high value is to be contrasted to an EA value of 2.86 eV for Al_{13}, reported in an earlier study.[58] A value of 3.0 eV has been reported even in very recent publications,[59,60] all because of the low-energy tail resulted from hot Al_{13}^-. The sharp spectral onset in the present study made it relatively straightforward to determine the threshold, and it also implied that there are relatively small geometry changes between the anion and the neutral ground states, justifying the above procedure to extrapolate the ADEs. Although VDEs are usually reported when poorly resolved PES data are obtained, this is only possible when a single electronic transition can be clearly resolved near the threshold. However, this is not possible for most TM clusters, which have an extremely high density of electronic states near the Fermi level. In that case, the VDEs determined might be rather arbitrary, because the PES band shape may change at different photon energies due to the fact that different detachment channels may have different photon-energy-dependent detachment cross sections. Therefore, we argue that ADEs represent a more consistent and reliable set of experimental observables when sharp PES onsets can be obtained.

IV. DISCUSSION

The PES spectra shown in Figs. 2–4 represent photodetachment transitions from the ground states or low-lying isomers of Ni_n^- cluster anions to the ground and low-lying excited states of Ni_n neutral clusters. A quantitative understanding of these data will require detailed theoretical calculations, not only on the neutral clusters, but also on the anions. Even under the current improved experimental conditions, very little fine structure was resolved in the PES spectra except for the very small ones, reflecting the intrinsic high density of electronic states in these systems, largely due to the open $3d$ shell. The complicated nature of the electronic structure of these systems makes it extremely challenging for high level theoretical calculations. Nevertheless, considerable theoretical efforts have been directed at under-

TABLE I. Adiabatic electron affinities (EA) in eV of Ni_n clusters.

n	EA	n	EA	n	EA
1	1.16±0.06[a]	30	2.88±0.05	59	3.32±0.05
2	0.85±0.10[b]	31	2.92±0.05	60	3.30±0.05
3	1.44±0.06[c]	32	2.94±0.05	61	3.33±0.05
4	1.50±0.06	33	2.93±0.05	62	3.35±0.05
5	1.57±0.06	34	2.97±0.05	63	3.34±0.05
6	1.87±0.05	35	3.04±0.05	64	3.36±0.05
7	1.86±0.05	36	3.04±0.05	65	3.36±0.05
8	1.97±0.05	37	3.05±0.05	66	3.38±0.05
9	1.96±0.05	38	3.08±0.05	67	3.40±0.05
10	2.06±0.05	39	3.08±0.05	68	3.35±0.05
11	2.06±0.05	40	3.10±0.05	69	3.36±0.05
12	2.09±0.05	41	3.11±0.05	70	3.36±0.05
13	2.16±0.05	42	3.14±0.05	71	3.38±0.05
14	2.28±0.05	43	3.13±0.05	72	3.36±0.05
15	2.37±0.05	44	3.15±0.05	73	3.40±0.05
16	2.40±0.05	45	3.19±0.05	74	3.42±0.05
17	2.50±0.05	46	3.16±0.05	75	3.44±0.05
18	2.51±0.05	47	3.19±0.05	76	3.45±0.05
19	2.51±0.05	48	3.17±0.05	77	3.44±0.05
20	2.59±0.05	49	3.20±0.05	78	3.40±0.05
21	2.58±0.05	50	3.20±0.05	79	3.42±0.05
22	2.61±0.05	51	3.19±0.05	80	3.36±0.05
23	2.65±0.05	52	3.20±0.05	82	3.42±0.05
24	2.67±0.05	53	3.21±0.05	85	3.45±0.05
25	2.71±0.05	54	3.24±0.05	90	3.45±0.05
26	2.73±0.05	55	3.27±0.05	95	3.48±0.05
27	2.75±0.05	56	3.25±0.05	100	3.52±0.05
28	2.73±0.05	57	3.28±0.05		
29	2.84±0.05	58	3.28±0.05		

[a]1.15716±0.000 12 eV from Ref. 54.
[b]0.926±0.010 eV from Ref. 47.
[c]For the triangular isomer; 1.41±0.05 eV from Ref. 48. For the linear isomer, the EA was determined to be 1.86±0.05 eV.

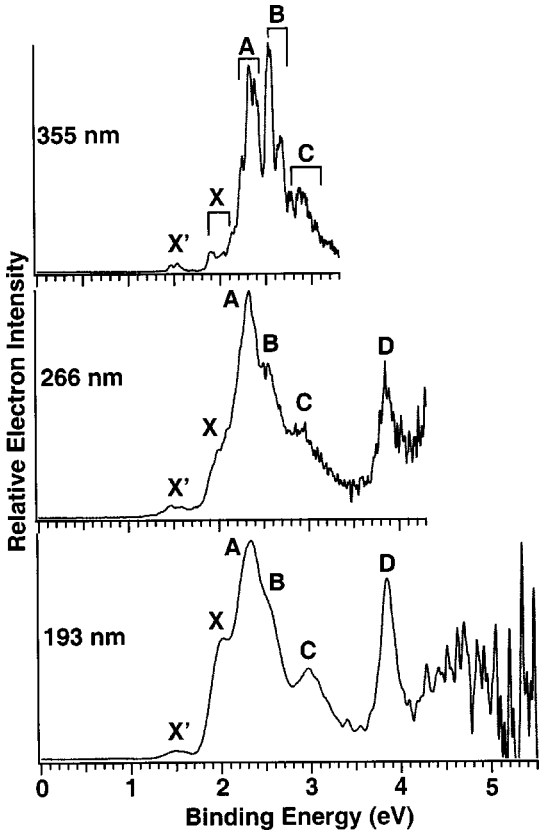

FIG. 6. Photoelectron spectra of Ni_3^- at three different photon energies.

standing small Ni clusters,[23–44] mostly on the neutral systems. Recently, Jena and co-workers have studied several anion Ni_n^- clusters ($n=3,5,7$) and used the available PES data effectively to provide insight into the structures and magnetic moments of small Ni clusters.[29–31] They showed that well-resolved PES data are highly valuable to verify various theoretical methods for the complicated TM cluster systems. They also showed that low-lying isomers are very common, not only for the neutral clusters, but also for the anions, which might be populated in the PES experiments. In the next section, we will present evidence of two possible isomers in Ni_3^-. Then, we will mainly focus our discussion on the trend and evolution of the PES data and attempt to correlate changes of the PES spectra to other properties of Ni clusters.

A. Ni_3^-: Coexistence of two isomers

Figure 6 displays the Ni_3^- spectra at three detachment photon energies. The 193 nm spectrum showed five intense bands (X,A–D) between 1.7 and 4.1 eV binding energies with a very weak band (X′) at the lowest binding energy. There also seemed to be real signals beyond 4.1 eV, but the signal-to-noise ratio was poor in the high binding energy side. At 266 nm, the intensity of the X band was reduced and the A and B bands were slightly better resolved. At 355 nm, the intensity of the X band was further reduced and that of the B band was increased. But more significantly, all bands were considerably better resolved at 355 nm; each was resolved into numerous fine features, as indicated. These fine features could be due to vibrational excitations, but more likely due to low-lying electronic states of neutral Ni_3. The PES spectrum of Ni_3^- was reported previously at 488 nm by Ervin *et al.* at a higher instrumental resolution.[48] The spectrum at 488 nm, which seemed to be broader, corresponds to the X′ and X bands in the current data and missed the intense features at higher binding energies.

We observed that the intensity of the X band strongly depended on the detachment photon energies, and to a smaller degree that of the B band as well. This photon-energy-dependent behavior is common in PES, reflecting the nature of the electrons detached. However, the X′ band was very weak at all three detachment photon energies. Its independence on photon energies and its feeble intensity suggested that it did not belong to the group of intense bands (X,A–D). Rather, it was likely due to a minor isomer. The X′ band gives an ADE of 1.44±0.06 eV for the minor isomer. This value agrees well with that (1.41±0.05 eV) obtained by Ervin *et al.*[48] The X band yields an ADE of 1.86±0.05 eV for the major isomer.

Indeed, Jena *et al.* predicted that Ni_3^- has two almost degenerate isomers: a linear one and a triangular one, each with a quartet spin multiplicity ($M=4$).[29] However, the triangular structure is more stable in the neutral, indicating that the detachment energies from the triangular isomer would be lower. The calculated ADEs for the triangular and linear iso-

mers are 0.97 and 2.03 eV, respectively.[29] Although the calculated values are off by as much as 0.4 eV for the triangular isomer, qualitatively the theoretical results are in good agreement with our observation. Therefore, we attribute the major observed bands (X,A–D) to the linear isomer. In light of the current results, it seems that higher levels of calculations would be highly desirable on the Ni trimer systems.

B. Possible structure effects revealed by PES data

In this section, we examine the PES spectral changes and attempt to correlate these changes with possible cluster structural changes. As shown in Fig. 2, the very small clusters ($n \leqslant 6$) exhibit very strong size dependence, implying that these clusters are molecule-like with different electronic and geometrical structures. Ni_{10}^-, Ni_{11}^-, and Ni_{12}^- all possess a single broadband. An abrupt change from Ni_{12}^- to Ni_{13}^- was observed: the spectrum of Ni_{13}^- has a much sharper band compared to that of Ni_{12}^-. This result is very similar to that observed in the Al, Ti, and Co clusters.[56,61,62] The 12-atom clusters for these systems all give a broad PES band, but the PES spectra of the 13-atom clusters abruptly become a much narrower band. This dramatic change is attributed to a structure change from a less symmetrical arrangement of 12 atoms to a highly symmetric icosahedral structure for the 13-atom clusters. The high symmetry of the I_h clusters leads to a higher degree of electronic degeneracy, and consequently a narrower PES band.[52] The spectra of Ni_{14}^- and Ni_{15}^- appear similar to that of Ni_{13}^-, suggesting that their structures may follow the icosahedral packing by simply attaching the extra atoms on the surface of the 13-atom cluster, as are the cases for Al_{14}^- and Al_{15}^-.[52] This conclusion is consistent with results previously proposed based on chemisorption experiments, magnetic experiments, and theoretical calculations.

The spectrum of Ni_{19}^- shows a partially resolved shoulder in the threshold region. No such features were observed for either Ni_{18}^- or Ni_{20}^-. This observation may indicate a more symmetric structure for Ni_{19}^-, consistent with the double icosahedral structure previously proposed for Ni_{19} from the chemical absorption experiment and theoretical calculations.[3,24] For Ni_{23}^-, a very sharp peak was resolved in the threshold, again, indicating possibly a more symmetric cluster. Indeed, Ni_{23} has been proposed to possess a triple icosahedron structure with D_{3h} symmetry.[3,24] The partially resolved threshold peak in the spectra of Ni_{22}^- to Ni_{26}^- indicate that they may possess similar structures as Ni_{23} by removing one atom from or adding one to three atoms to the triple icosahedral surface of Ni_{23}.

The PES spectra between Ni_{30}^- to Ni_{100}^- are all broad and featureless, except around Ni_{55}^-, where a sharp peak was resolved near the threshold for clusters of $n=54-61$. The sharp threshold feature gradually disappeared in the large cluster regime beyond Ni_{62}^-. This abrupt PES spectral change was attributed to a highly symmetric double-shell icosahedral structure for Ni_{55}^- and the icosahedral packing around this size. Similar PES results were also obtained previously for Ti_{55}^- and Co_{55}^-.[61,62] This observation is consistent with an icosahedral structure previously suggested for Ni_{55} from both the chemsorption and magnetic experiments.[4,14] An I_h-Ni_{55} has also been used in previous theoretical studies on its electronic and magnetic properties.

Recently, the electric dipole polarizabilities of neutral Ni clusters from Ni_{12} to Ni_{58} have been measured by Knickelbein.[63] Local minima at Ni_{13}, Ni_{19}, Ni_{23}, Ni_{24}, and Ni_{55} and maxima around Ni_{22}, Ni_{25}, and Ni_{51} were observed and correlated with the cluster structures. High symmetry clusters are expected to be less polarizable relative to clusters with low symmetry. The current PES results are consistent with these observations.

C. Correlation of electronic structure and magnetic properties of Ni cluster

The ground state electron configuration of the Ni atom is $3d^8 4s^2$. In small Ni clusters or the bulk, it assumes a configuration of $3d^9 4s^1$, which is only 0.025 eV higher in energy than the ground state.[54] The *s* electrons provide the chemical bonding primarily and the *d* electrons are mainly localized to their atomic cores. Although the *s* bonding electrons make a contribution to the magnetic moments, the large magnetic moments of small clusters are mainly resulted from the localized and unpaired *d* electrons, which are coupled according to the Hund's rule. For Ni atom with a configuration of $3d^9 4s^1$, one *d* electron is unpaired. According to the superparamagnetic model for small ferromagnetic clusters, the atomic magnetic moments are ferromagnetically aligned to form a single magnetic domain in a cluster.[64] Thus, the behavior of the *d* electrons governs the electronic states and the magnetic moments of these clusters.

Based on the similarity of the PES spectra of Cu and Ni, for clusters up to $n=6$, Gantefor and Eberhardt concluded that there is very little s/d hybridization in the small Ni clusters, resulting in their enhanced magnetic moments.[45] The current data further revealed similar spectral features for Ni_6^- to Ni_9^- (Fig. 2). All the spectra possess a sharp peak at the threshold and a broadband at higher binding energies. The resolved sharp peak for Ni_7^- and Ni_9^- are comparable to that of Cu_7^- and Cu_9^-.[45] This resemblance suggests that the *d* electrons in Ni_7 and Ni_9 are still largely localized and the resolved sharp peaks come primarily from the *s* electrons. Figure 2 showed that the spacing between the first peak and the broadband decreases gradually with the increase of the cluster size and disappears at Ni_{10}. The merge of this sharp peak to the broadband at Ni_{10}^- indicates significant delocalization of the $3d$ electrons and the onset of s/d hybridization, which is expected to cause a significant reduction in the magnetic moments of the clusters. Indeed, the magnetic moment of Ni clusters has been found to show a dramatic decrease with cluster size from Ni_5 to Ni_{10}, and the value at Ni_{10} reaches a level comparable to a wide plateau around Ni_{18}. A local minimum at Ni_{13} was also observed, which was attributed to a highly symmetric icosahedral structure, as discussed above. We observed similar PES spectral behaviors in small Co clusters previously and were also able to correlate well with their magnetic moment changes with cluster size.[65]

In the current study, we further confirmed that the sharp and intense threshold features in small Ni_n^- clusters were indeed due to the detachment of $4s$ electrons by examining

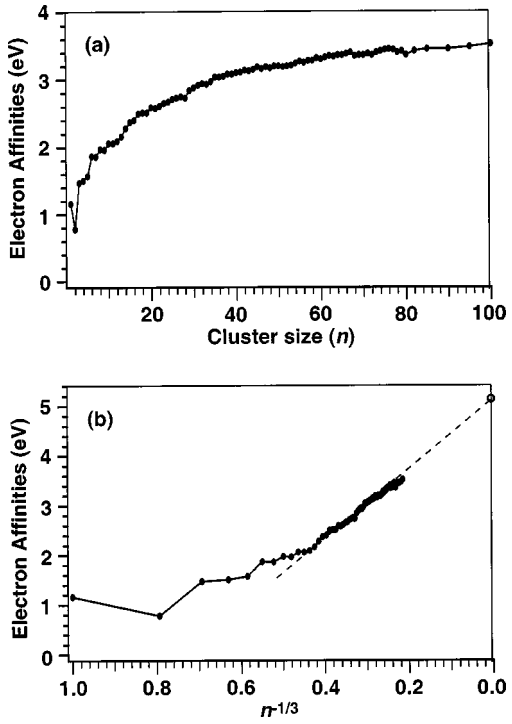

FIG. 7. (a) Electron affinities (EA) of Ni_n ($n=1-100$) as a function of size n. (b) EA vs $n^{-1/3}$ ($n^{-1/3}$ is proportional to $1/r$, r being the cluster radius).

the spectra of the atoms and photon-energy-dependent spectra. As seen from the spectrum of Ni^- in Fig. 2 at 355 nm, the detachment cross sections of s electrons are much higher than that of d electrons. In fact, the detachment features from d electrons in Ni^- near the threshold were not even visible because they were completely overwhelmed by the features from the detachment of the s electrons. This observation suggests that the sharp and intense features in the 355 nm PES spectra of the clusters ($n \leqslant 9$) should also primarily be due to the detachment of $4s$ electrons. The detachment cross sections for the d electrons were expected to increase with photon energy and the intensity of the s features should decrease at higher photon energies.[55] Indeed, we found that the intensities of all the sharp PES peaks in the Ni_n^- clusters decreased at higher photon energies (Fig. 5). This observation confirmed unequivocally that the sharp peaks near the threshold in the small Ni clusters were due to the detachment of mainly s electrons. The congested features at higher binding energies are consistent with detachment from the open-shell $3d$ levels.

D. Electron affinity versus cluster size

The EA values are plotted in Fig. 7 as a function of cluster size. Large size variation is observed for small clusters of $n<10$. Ni_2 exhibits the lowest EA value. Beyond $n=10$, the EA gradually increases with increasing cluster size. A classical metallic droplet model is used to describe the evolution of the EAs as a function of cluster size.[66] According to this model, the EA of a particle with a radius, r, is linearly dependent on $1/r$. Figure 7(b) shows that for $n>10$ the EAs indeed follow a straight line, which extrapolates to a value of ~5.1 eV at an infinite cluster size. Within the experimental uncertainty, this value is consistent with the bulk work function of nickel (~5.19 eV), suggesting that Ni clusters become metallic above about Ni_{10}. This is corroborated by their nearly continuous density of states starting at this size.

V. CONCLUSIONS

We report a comprehensive PES study of Ni_n^- clusters ($n=1-100$) at three photon energies with special attention to cluster temperatures. Sharp threshold features were observed and allowed us to obtain the EAs more accurately. Evidence was presented for the existence of two isomers for Ni_3^-; a minor triangular one and a main linear isomer. Abrupt spectral changes were observed from Ni_{12}^- to Ni_{13}^- and also around Ni_{55}^- and were correlated to the high symmetry icosahedral structures proposed for Ni_{13} and Ni_{55}. Similar geometric effects on the PES spectra for Ni_{19}^- and Ni_{23}^- were also observed, which were previously proposed to have double and triple icosahedral structures, respectively. The evolution of the electronic structure of Ni clusters as a function of size is clearly revealed. The high density of electronic states in the Ni systems yielded highly congested PES spectra. For small clusters, a sharp spectral feature, mainly due to the detachment of $4s$ electrons as revealed by the photon-energy-dependent studies, was observed to overlap with the primarily $3d$ features at Ni_{10}^-, indicating the onset of significant $s-d$ hybridization at this size. This observation is consistent with the trend of magnetic moments measured for small Ni clusters and the onset of metallic behavior.

ACKNOWLEDGMENTS

This work was supported by the National Science Foundation (Grant No. CHE-9817811) and performed at the W. R. Wiley Environmental Molecular Science Laboratory, a national scientific user facility sponsored by the Department of Energy's (DOE's) Office of Biological and Environmental Research and located at the Pacific Northwest National Laboratory, operated for the DOE by Battelle.

[1] E. K. Parks, B. J. Winter, T. D. Klots, and S. J. Riley, J. Chem. Phys. **94**, 1882 (1991).
[2] E. K. Parks, L. Zhu, J. Ho, and S. J. Riley, J. Chem. Phys. **100**, 7206 (1994).
[3] E. K. Parks, L. Zhu, J. Ho, and S. J. Riley, J. Chem. Phys. **102**, 7377 (1995).
[4] E. K. Parks and S. J. Riley, Z. Phys. D: At., Mol. Clusters **33**, 59 (1995).
[5] E. K. Parks, G. C. Nieman, K. P. Kerns, and S. J. Riley, J. Chem. Phys. **107**, 1861 (1997).
[6] E. K. Parks, K. P. Kerns, and S. J. Riley, J. Chem. Phys. **109**, 10207 (1998).
[7] E. K. Parks, K. P. Kerns, and S. J. Riley, J. Chem. Phys. **112**, 3384 (2000).
[8] K. P. Kerns, E. K. Parks, and S. J. Riley, J. Chem. Phys. **112**, 3394 (2000).
[9] E. K. Parks, K. P. Kerns, and S. J. Riley, J. Chem. Phys. **114**, 2228 (2001).
[10] E. K. Parks, G. C. Nieman, and S. J. Riley, J. Chem. Phys. **115**, 4125 (2001).
[11] M. Pellarin, B. Baguenard, J. L. Vialle, J. Lerme, M. Broyer, J. Miller, and A. Perez, Chem. Phys. Lett. **217**, 349 (1994).
[12] I. M. L. Billas, A. Chatelain, and W. A. de Heer, Science **265**, 1682 (1994).
[13] I. M. L. Billas, A. Chatelain, and W. A. de Heer, J. Magn. Magn. Mater. **168**, 64 (1997).
[14] S. E. Aspel, J. W. Emmer, J. Deng, and L. A. Bloomfield, Phys. Rev. Lett. **76**, 1441 (1996).

[15] M. B. Knickelbein, J. Chem. Phys. **116**, 9703 (2002).
[16] M. B. Knickelbein, S. Yang, and S. J. Riley, J. Chem. Phys. **93**, 94 (1990).
[17] J. Jellinek and I. L. Garzon, Z. Phys. D: At., Mol. Clusters **26**, 110 (1993).
[18] P. Durmus, M. Boyukata, S. Ozcelik, Z. B. Guvenc, and J. Jellinek, Surf. Sci. **454**, 310 (2000).
[19] R. Fournier, M. S. Stave, and A. E. Depristo, J. Chem. Phys. **96**, 1530 (1992).
[20] B. Chen, M. A. Gomez, M. Sehl, J. D. Doll, and D. L. Freeman, J. Chem. Phys. **105**, 9686 (1996).
[21] E. Curotto, A. Matro, D. L. Freeman, and J. D. Doll, J. Chem. Phys. **108**, 729 (1998).
[22] F. Liu, R. Liyanage, and P. B. Armentrout, J. Chem. Phys. **117**, 132 (2002).
[23] C. L. Cleveland and U. Landman, J. Chem. Phys. **94**, 7376 (1991).
[24] M. S. Stave and A. E. Depristo, J. Chem. Phys. **97**, 3386 (1992).
[25] T. L. Wetzel and A. E. DePristo, J. Chem. Phys. **105**, 572 (1996).
[26] J. M. Montejano-Carrizales, M. P. Iniguez, J. A. Alonso, and M. J. Lopez, Phys. Rev. B **54**, 5961 (1996).
[27] F. Ruette and C. Gonzalez, Chem. Phys. Lett. **359**, 428 (2002).
[28] F. A. Reuse, S. N. Khanna, and S. Bernel, Phys. Rev. B **52**, 11650 (1995).
[29] S. E. Weber and P. Jena, Chem. Phys. Lett. **281**, 401 (1997).
[30] S. N. Khanna and P. Jena, Chem. Phys. Lett. **336**, 467 (2001).
[31] S. N. Khanna, M. Beltran, and P. Jena, Phys. Rev. B **64**, 235419 (2001).
[32] B. V. Reddy, S. K. Nayak, S. N. Khanna, B. K. Rao, and P. Jena, J. Phys. Chem. A **102**, 1748 (1998).
[33] S. Bouarab, A. Vega, M. J. Lopez, M. P. Iniguez, and J. A. Alonso, Phys. Rev. B **55**, 13279 (1997).
[34] F. Aguilera-Granja, S. Bouarab, M. J. Lopez, A. Vega, J. M. Montejano-Carrizales, M. P. Iniquez, and J. A. Alonso, Phys. Rev. B **57**, 12469 (1998).
[35] N. N. Lathiotakis, A. N. Andriotis, M. Menon, and J. Connolly, J. Chem. Phys. **104**, 992 (1996).
[36] A. N. Andriotis and M. Menon, Phys. Rev. B **57**, 10069 (1998).
[37] G. M. Pastor, R. Hirsch, and B. Muhlschlegel, Phys. Rev. B **53**, 10382 (1996).
[38] M. Castro, C. Jamorski, and D. R. Salahub, Chem. Phys. Lett. **271**, 133 (1997).
[39] G. A. Cisneros, M. Castro, and D. R. Salahub, Int. J. Quantum Chem. **75**, 847 (1999).
[40] S. Kruger, T. J. Seemuller, A. Worndle, and N. Rosch, Int. J. Quantum Chem. **80**, 567 (2000).
[41] G. L. Estin and M. C. Zerner, J. Phys. Chem. **100**, 16874 (1996).
[42] N. Fujima and T. Yamaguchi, Phys. Rev. B **54**, 26 (1996).
[43] H. M. Duan, X. G. Gong, Q. Q. Zheng, and H. Q. Lin, J. Appl. Phys. **89**, 7308 (2001).
[44] Y. Xiang, D. Y. Sun, and X. G. Gong, J. Phys. Chem. A **104**, 2746 (2000).
[45] G. Gantefor and W. Eberhardt, Phys. Rev. Lett. **76**, 4975 (1996).
[46] L. S. Wang and H. B. Wu, Z. Phys. Chem. (Munich) **203**, 45 (1998).
[47] J. Ho, M. L. Polak, K. M. Ervin, and W. C. Lineberger, J. Chem. Phys. **99**, 8542 (1993).
[48] K. M. Evin, J. Ho, and W. C. Lineberger, J. Chem. Phys. **89**, 4514 (1988).
[49] J. A. Alonso, Chem. Rev. **100**, 637 (2000).
[50] L. S. Wang, H. S. Cheng, and J. Fan, J. Chem. Phys. **102**, 9480 (1995).
[51] L. S. Wang and H. Wu, in *Advances in Metal and Semiconductor Clusters*, Vol. 4, Cluster Materials, edited by M. A. Duncan (JAI, Greenwich, 1998), p. 299.
[52] J. Akola, M. Manninen, H. Hakkinen, U. Landman, X. Li, and L. S. Wang, Phys. Rev. B **60**, 11297 (1999).
[53] L. S. Wang and X. Li, *Clusters and Nonostructure Interfaces*, edited by P. Jena, S. N. Khanna, and B. K. Rao (World Scientific, CHY, Singapore, 2000), p. 293.
[54] M. Scheer, C. A. Brodie, R. C. Bilodeau, and H. K. Haugen, Phys. Rev. A **58**, 2051 (1998).
[55] S. Hufner, *Photoelectron Spectroscopy* (Spring-Verlag, New York, 1995), p. 15.
[56] X. Li, H. Wu, X. B. Wang, and L. S. Wang, Phys. Rev. Lett. **81**, 1909 (1998).
[57] X. Li and L. S. Wang, Phys. Rev. B **65**, 153404 (2002).
[58] K. J. Tarlor, C. L. Pettiette, M. J. Craycraft, O. Chesnovsky, and R. E. Smalley, Chem. Phys. Lett. **152**, 347 (1988).
[59] H. Kawamata, Y. Negishi, A. Nakajima, and K. Kaya, Chem. Phys. Lett. **337**, 255 (2001).
[60] A. Pramann, A. Nakajima, and K. Kaya, J. Chem. Phys. **115**, 5404 (2001).
[61] H. Wu, S. R. Desai, and L. S. Wang, Phys. Rev. Lett. **76**, 212 (1996).
[62] S. R. Liu, H. J. Zhai, and L. S. Wang, Phys. Rev. B **64**, 153402 (2001).
[63] M. B. Knickelbein, J. Chem. Phys. **115**, 5957 (2001).
[64] S. N. Khanna and S. Linderoth, Phys. Rev. Lett. **67**, 742 (1991).
[65] S. R. Liu, H. J. Zhai, and L. S. Wang, Phys. Rev. B **65**, 113401 (2002).
[66] D. M. Wood, Phys. Rev. Lett. **46**, 749 (1981).